VNU Journal of Science: Mathematics - Physics

Journal homepage: https://js.vnu.edu.vn/MaP

Original Article

Electric Field-induced Semiconductor-to-Semimetal Transition in Monolayer Bi_2C_3: A First-Principles Investigation

Nguyen Van Chuong[1,*], Pham Thiet Truong[2], Le Thi Hoa[3], Tran Ngoc Bich[4], Huynh Vinh Phuc[2], Nguyen Van Hieu[2], Nguyen Ngoc Hieu[5]

[1]*Le Quy Don Technical University, 236 Hoang Quoc Viet, Nghia Do, Ha Noi, Vietnam*

[2]*Dong Thap University, 783 Pham Huu Lau, Cao Lanh, Dong Thap, Vietnam*

[3] *University of Science and Education, University of Danang, 459 Ton Duc Thang, Hoa Khanh, Da Nang, Vietnam*

[4]*VN-UK Institute for Research and Executive, University of Danang Education, 158A Le Loi, Hai Chau, Da Nang, Vietnam*

[5]*Duy Tan University, 254 Nguyen Van Linh, Thanh Khe, Da Nang, Vietnam*

Received 4th September 2025
Revised 15h October 2025; Accepted 2nd March 2026

Abstract: In this work, we perform comprehensive first-principles calculations to investigate the structural, mechanical, electronic, optical, and field-tunable properties of a newly proposed two-dimensional (2D) material, monolayer Bi_2C_3. Structural optimization and phonon spectrum analysis confirm its dynamical stability. The Bi_2C_3 monolayer adopts a buckled honeycomb-like configuration, characterized by strong C-C sp^2 bonding and Bi-C sp^3 hybridization. Our analysis of its mechanical properties reveals significant anisotropy, with a maximum Young's modulus of 28.85 N/m. Monolayer Bi_2C_3 is an indirect semiconductor, with a PBE/HSE06 band gap of 0.82/1.37 eV. Furthermore, the material exhibits strong and broad light absorption, spanning from the visible to the ultraviolet region, with a maximum absorption coefficient of 6.50×10^5 cm^{-1}. Most importantly, we demonstrate that the band gap of Bi_2C_3 can be effectively tuned by applying a perpendicular electric field. This electric field induces a progressive reduction in the band gap, ultimately driving a semiconductor-to-semimetal transition. These findings demonstrate that monolayer Bi_2C_3 is a dynamically stable 2D semiconductor with highly tunable electronic and optical properties, positioning it as a promising candidate for next-generation electronic and optoelectronic applications.

Keywords: Two-dimensional materials, First-principles calculations, Monolayer Bi_2C_3, Electronic properties, Electric field tunable.

* Corresponding author.
E-mail address: chuong.vnguyen@lqdtu.edu.vn

https//doi.org/10.25073/2588-1124/vnumap.5075

1. Introduction

Since the successful isolation of graphene in 2004 [1], two-dimensional (2D) materials have attracted tremendous attention due to their unique physical and chemical properties. Graphene, a monolayer of sp^2-bonded carbon atoms arranged in a honeycomb lattice, exhibits exceptional electronic properties [2]. These remarkable features have sparked intensive research efforts into graphene and its potential applications in next-generation applications [3-5]. However, despite its outstanding properties, graphene also suffers from several intrinsic limitations. Most notably, its zero band gap hinders its direct application in semiconductor devices that require an on-off switching capability. Additionally, challenges in large-scale synthesis and integration have motivated researchers to explore beyond graphene for alternative 2D materials with more versatile properties. Recently, a wide variety of 2D materials have been proposed and investigated, including transition metal dichalcogenides (TMDs) [6], phosphorene [7] and MXenes [8]. These materials not only extend the family of 2D systems but also provide tunable properties, offering promising pathways for novel device applications. Among them, MoS_2 has emerged as a representative TMD semiconductor. Monolayer MoS_2 possesses a direct band gap of approximately 1.8 eV, making it a promising candidate for electronic and optoelectronic devices [9]. Nevertheless, its relatively low carrier mobility of about 200 $cm^2V^{-1}s^{-1}$) restricts its applicability in high-speed devices [10]. Phosphorene, an atomically thin layers of phosphorus exfoliated from black phosphorus, has been considered another ideal candidate due to its inherent direct band gap (~2.0 eV) and high hole mobility on the order of 10^3 $cm^2V^{-1}s^{-1}$ [11]. However, few-layer phosphorene-based devices suffer from severe environmental instability when exposed to ambient conditions and can only operate reliably in inert atmospheres [12]. Thus, scientists have continued to search for novel 2D materials that combine tunable band gaps, high carrier mobility, and robust environmental stability.

Recently, Liu et al., [13], based on first-principles calculations, proposed a novel class of 2D materials, M_2C_3 (M = As, Sb, Bi). These materials enrich the library of emerging 2D systems and are predicted to possess promising electronic characteristics, thereby opening new opportunities for nanoelectronic and optoelectronic applications. Nguyen et al., [14] predicted that monolayer As_2C_3 could be utilized as a promising channel material when integrated with 2D metallic goldene, suggesting novel device architectures with enhanced electronic performance. Kumar et al., [15] demonstrated that monolayer Sb_2C_3 can serve as an efficient sensor for environmentally toxic nitrogen-containing gases. Despite these advances, the monolayer form of Bi_2C_3 remains significantly underexplored. A systematic investigation into its fundamental electronic, mechanical andd optical properties is critically lacking, which hinders its potential for practical applications. Therefore, this work employs first-principles calculations to comprehensively investigate the atomic structure, stability, and electronic and optical properties of monolayer Bi_2C_3 as well as the tunability of its properties under applied electric fields. Our findings aim to provide crucial guidance for the practical application of semiconducting Bi_2C_3 in next-generation switching devices.

2. Computational Methods

First-principles calculations based on density functional theory (DFT) were carried out using the Vienna Ab initio Simulation Package (VASP) [16]. The interaction between ion cores and valence electrons was described by the projector augmented wave (PAW) method [17]. For the exchange-correlation functional, the generalized gradient approximation (GGA) in the Perdew-Burke-Ernzerhof (PBE) functional [18] was employed. To obtain more accurate electronic band structures, the Heyd-Scuseria-Ernzerhof (HSE06) hybrid functional [19] was additionally used. A plane-wave cutoff energy of 510 eV was applied throughout all calculations. The Brillouin zone was sampled using a Monkhorst-

Pack k-point mesh of 15 × 15 × 1 for geometry optimizations and electronic property calculations. A vacuum region of 20 Å was introduced along the out-of-plane direction to avoid spurious interactions between periodic images. All atomic structures were fully relaxed until the residual force on each atom was less than 0.01 eV/Å and the total energy was converged to within 10^{-6} eV. The phonon dispersion spectra were calculated using the Density Functional Perturbation Theory (DFPT) to confirm the dynamical stability of the optimized structures.

3. Results and Discussion

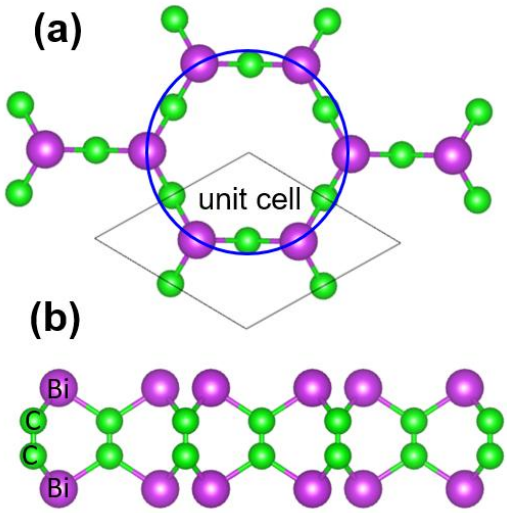

Figure 1. (a) Top view and (b) side view of the optimized atomic structures of monolayer Bi_2C_3.

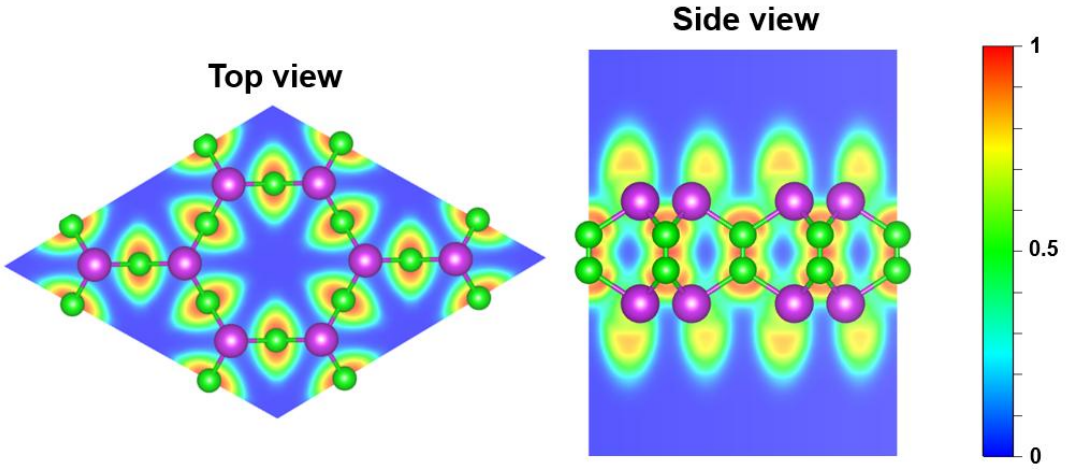

Figure 2. Top view and side view of the electron localization function (ELF) of monolayer Bi_2C_3. The ELF ranges from 0 to 1, with 0 denoting no electron, 0.5 indicating electron-gas-like pair, and 1 signifying complete localization.

Figure 1 presents the atomic structure of monolayer Bi_2C_3 after full geometric optimization. The Bi_2C_3 monolayer adopts a buckled honeycomb-like configuration with a layered arrangement. Each unit cell contains four Bi atoms and six C atoms. Within the hexagonal framework, each Bi atom is coordinated with three neighboring C atoms, while each C atom bonds to two Bi atoms, forming a stable covalent network. The lattice constant of monolayer Bi_2C_3 is found to be 6.68 Å, which is in good agreement with that obtained in the previous reports [13, 20], thereby confirming the reliability of our computational approach. The vertical C-C and Bi-C bond lengths are measured to be 1.32 and 2.30 Å, respectively. It should be noted that the C-C bond length is comparable with that in other M_2C_3 (M = As, Sb) monolayers [13] but it is smaller than that in ideal graphene (1.42 Å) [21]. Furthermore, to evaluate the bonding characteristics of monolayer Bi_2C_3, we calculate its electron localization function (ELF), as illustrated in Figure 2. The results clearly indicate that the C-C bonds are strong and exhibit typical sp^2 bonding characteristics, with ELF values between the C-C atoms exceeding 0.5. In contrast, the Bi-C bonds are mainly associated with localization between sp^2 and sp^3 hybridization, reflecting the mixed covalent nature of the bonding within the Bi_2C_3 monolayer.

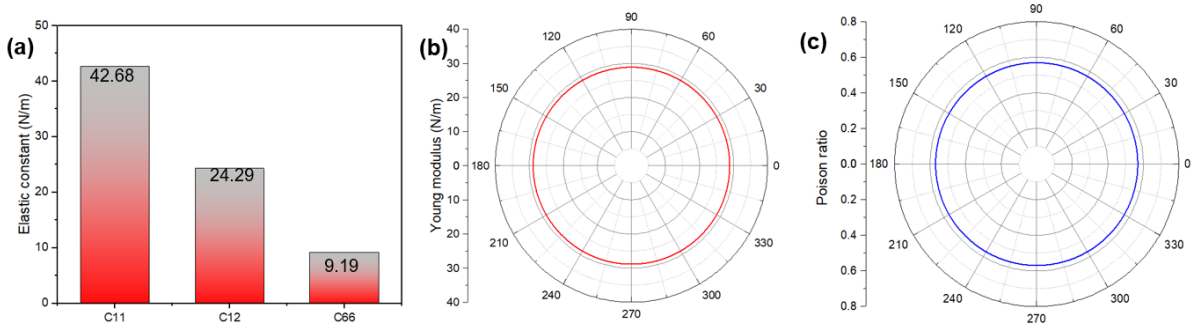

Figure 3. (a) Elastic constants, the angular depenecence of (b) Young's modulus and (c) Poison ratio of monolayer Bi_2C_3.

We further evaluate the stability of monolayer Bi_2C_3 by calculating the elastic constants and phonon dispersions curves and. The elastic constants of 2D monolayer Bi_2C_3 is calculated via the Hooke's law, which is derived from the energy-stress relationship. Due to a honeycomb structure, monolayer Bi_2C_3 contains three independent elastic components, including C_{11}, C_{12} and C_{66}. The calculated elastic constants C_{ij} of monolayer Bi_2C_3 are illustrated in Figure 3(a). One can find that the elastic constants of monolayer Bi_2C_3 fulfills the Bohn-Huang stability criteria [22, 23], i.e $C_{11} > |C_{12}|$ and $C_{66} > 0$. This indicates that the monolayer Bi_2C_3 is mechanical stability. Additionally, the Young's modulus is described the flexibility of material, thereby we further calculate the Young's modulus as a function of angles as follows:

$$E(\theta) = \frac{C_{11}^2 - C_{12}^2}{C_{11}\sin^4\theta + C_{22}\cos^4\theta + \left(\frac{C_{11}C_{22} - C_{12}^2}{C_{66}} - 2C_{12}\right)\cos^2\sin^2\theta} \quad (1)$$

It can be seen that monolayer Bi_2C_3 exhibits anisotropic mechanical properties. The Young's modulus of monolayer Bi_2C_3 (Figure 4(b)) reaches a maximum value of 28.85 N/m, which is significant smaller than that of graphene and phosphorene [24, 25]. This suggests that although Bi_2C_3 is mechanically softer than other 2D materials and it still possesses sufficient in-plane stiffness for practical applications, while potentially offering higher structural flexibility. The Posion ratio of monolayer Bi_2C_3

is measured to be 0.52, as shown in Figure 4(c). This value is comparable with that in other 2D materials [26], indicating that monolayer Bi_2C_3 possesses high mechanical flexibility and strong resistance to deformation under external strain.

The dynamical stability of the Bi_2C_3 monolayer was examined through AIMD simulations and further confirmed by its phonon spectrum, as illustrated in Figure 4. As can be seen, no imaginary frequencies are observed in the phonon dispersion, thereby validating the dynamical stability of the Bi_2C_3 monolayer.

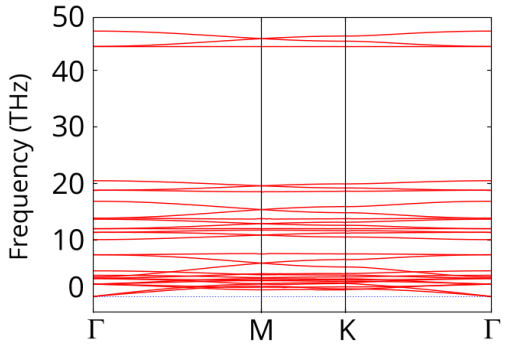

Figure 4. Phonon dispersion curves of monolayer Bi_2C_3.

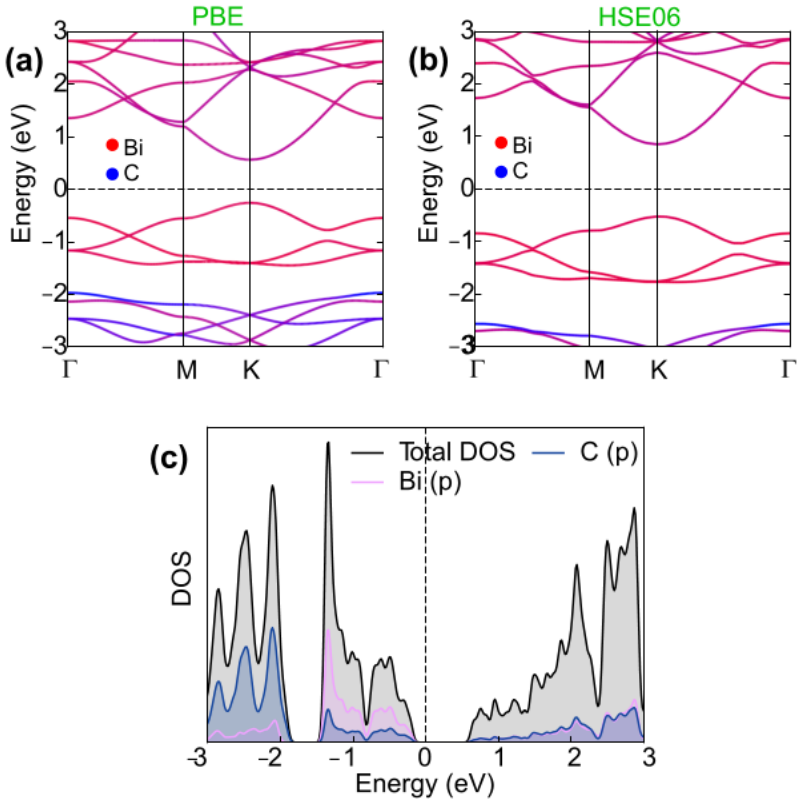

Figure 5. (a) PBE and (b) HSE06 projected band structures and density of states (DOS) of all atoms in monolayer Bi_2C_3.

The projected band structures of monolayer Bi_2C_3 are depicted in Figure 5. As shown in Figure 5(a), Bi_2C_3 exhibits semiconducting behavior with an indirect band gap of 0.82 eV, which is in good agreement with previous reports. In addition, the band gap of Bi_2C_3 monolayer is predicted to be smaller than that of other M_2C_3 (M = As, Sb) monolayers [13]. Both the valence band maximum (VBM) and conduction band minimum (CBM) are located at the K point and are predominantly contributed by the hybridization between Bi and C atoms. It is well known that the conventional PBE functional tends to underestimate the band gaps of 2D semiconductors. Therefore, we further employed the hybrid HSE06 functional to obtain a more accurate description of the electronic structure. The HSE06 results, presented in Figure 5(b), reveal an increased band gap, further confirming the semiconducting nature of the Bi_2C_3 monolayer. The calculated band gap of Bi_2C_3 monolayer is found to be 1.37 eV, which is significantly larger than the value obtained from the traditional PBE method. Nevertheless, the HSE06 calculations also predict an indirect band gap located at the K point, consistent with the PBE results. The consistency between the PBE and HSE06 results suggests that, despite the well-known underestimation of band gaps, the PBE functional still provides a reliable description of the electronic structure of Bi_2C_3 and can thus be employed in subsequent calculations. Given the reliability of the PBE functional in describing the electronic structure, we further calculate the density of states (DOS) of Bi_2C_3 to elucidate the contributions of individual atomic orbitals, as illustrated in Figure 5(c). The results indicate that the both the VBM and CBM of the Bi_2C_3 monolayer is primarily dominated by the Bi-p orbitals, with noticeable hybridization from the C-p orbitals.

Furthermore, we can calculate the optical absorption of the monolayer BiC3 as follows:

$$\alpha(\varpi) = \sqrt{2}\frac{\varpi}{c}\left[\sqrt{\varepsilon_1^2(\varpi)+\varepsilon_2^2(\varpi)} - \varepsilon_1(\varpi)\right]^{\frac{1}{2}}$$

The optical absorption of the Bi_2C_3 monolayer as a function of photon energy is depicted in Figure 6. The absorption coefficient is found to initiate in the visible region and extend into the ultraviolet region. A maximum optical absorption coefficient of 6.50 × 10^5 cm^{-1} for the Bi_2C_3 monolayer is observed at a photon energy of 4.2 eV. This value is comparable to or even higher than those reported for other 2D semiconductors, such as MoS_2 [27] and phosphorene [28]. Such strong and broad-range absorption suggests that the Bi_2C_3 monolayer is a promising candidate for next-generation nanoelectronic and optoelectronic devices, such as field-effect transistors (FETs) and UV photodetectors.

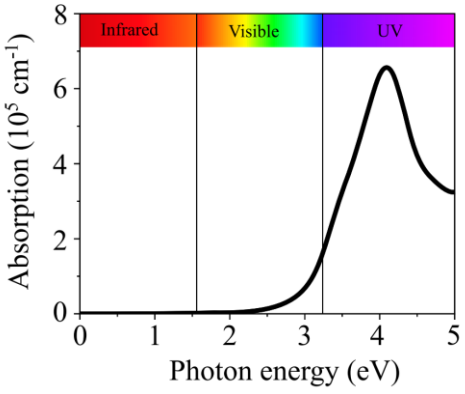

Figure 6. Optical absorption of monolayer Bi_2C_3 as a function of phonton energies.

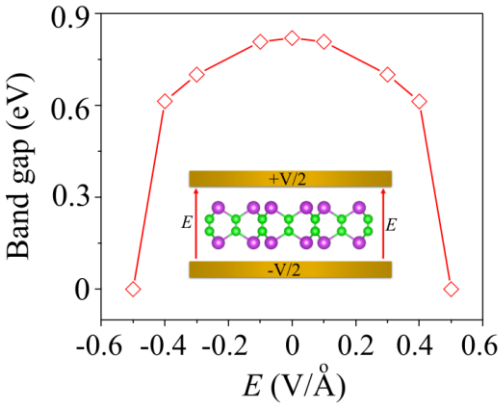

Figure 7. The evoluation of the band gap of Bi_2C_3 monolayer as a function of applied electric fields.

The application of an external electric field is a well-established strategy to effectively modulate the electronic properties of 2D materials. Previous studies have demonstrated that electric fields can induce band gap tuning and even trigger semiconductor-to-metal transitions in various 2D systems such as MoS_2 [29], black phosphorus [30], and 2D van der Waals heterostructure [31]. Motivated by these findings, we systematically investigate the influence of an external electric field on the electronic structure of the Bi_2C_3 monolayer. The electric field is applied perpendicularly to the Bi2C3 monolayer, as depicted in the inset of Figure 7. The direction of electric field pointing from bottom Bi layer to top Bi layer is defined as a positive direction. The evoluation of the band gaps of Bi_2C_3 monolayer as a function of the electric fields is illustrated in Figure 7. One can find that the band gap of the Bi_2C_3 monolayer exhibits a strong dependence on the strength and direction of the applied electric field. As the positive electric field increases, the band gap gradually decreases. Remarkably, when the field exceeds +0.6 V/Å, the band gap of Bi_2C_3 monolayer vanishes and the Bi_2C_3 monolayer undergoes a transition from a semiconductor to a semi-metallic state. A similar trend is observed under negative electric field. The application of a negative electric field also induces a continuous reduction in the band gap of the Bi_2C_3 monolayer. Under the negative electric field of -0.6 V/Å, the band gap vanishes entirely, signifying an electric field-driven semiconductor to semi-metal transition.

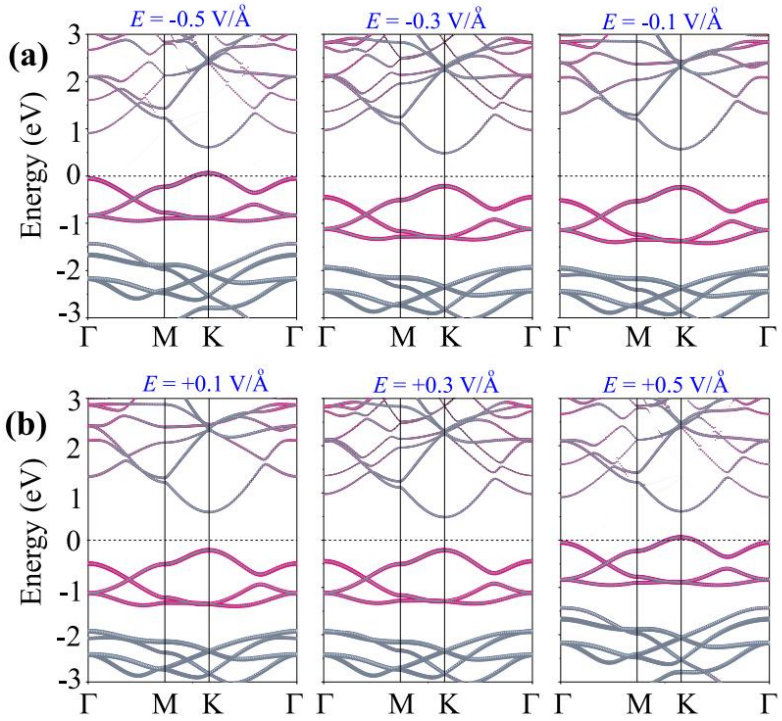

Figure 8. Projected band structures of the Bi_2C_3 monolayer under applied (a) positive and (b) negative electric fields. Purple and gray lines represent the contributions of the Bi and C atoms, respectively.

To gain a deeper understanding of the electric field's influence on the electronic properties of the Bi_2C_3 monolayer, we evaluated its projected band structures under various external fields. As illustrated in Figure 8, the application of an electric field effectively tunes the band gap by progressively shifting the band-edge states toward the Fermi level. Notably, the VBM of the semiconducting Bi_2C_3 shifts more rapidly toward the Fermi level than the CBM. This is because the VBM states are primarily composed of a strong hybridization between sp^2 and sp^3 of Bi-p and C-p orbitals. This orbital character makes them highly susceptible to external perturbations, such as an electric field, which preferentially lowers the potential energy of the electron-rich VBM states compared to the CBM states, which have a different orbital composition. Most remarkably, our calculations predict a semiconductor-to-semimetal transition at a negative electric field strength of -0.6 V/Å. At this critical field, the VBM at the K point crosses the Fermi level, effectively eliminating the band gap. Similarly, the application of a positive electric field also provides an effective method for tuning the electronic properties of the Bi_2C_3 monolayer. As illustrated in Figure 8(b), when a positive electric field is applied, both the VBM and the CBM of the semiconducting Bi_2C_3 monolayer shift toward the Fermi level. This results in a progressive decrease in the band gap. At a critical field strength of +0.6 V/Å, the VBM also crosses the Fermi level at the K point, which confirms the predicted semiconductor-to-semimetal transition. This result not only demonstrates a powerful method for precisely tuning the electronic properties of semiconductor Bi_2C_3 but also highlights its potential for applications in field-effect transistors (FETs) or other next-generation electronic switching devices.

4. Conclusion

In summary, we have performed a comprehensive first-principles study on the structural, mechanical, electronic, optical, and field-tunable properties of a newly proposed 2D material, monolayer Bi_2C_3. Our findings confirm that monolayer Bi_2C_3 is dynamically stable with a buckled honeycomb structure. We found that this material is an indirect semiconductor with a band gap of 0.82/1.37 eV predicted by PBE/HSE06 functional. The material exhibits strong and broadband light absorption in the visible and ultraviolet regions. Most significantly, our results demonstrate that the electronic properties of Bi_2C_3 can be effectively tuned by applying a perpendicular electric field. A field strength of ±0.6 V/Å induces a progressive reduction in the band gap, ultimately triggering a semiconductor-to-semimetal transition. This remarkable tunability highlights the potential of Bi_2C_3 for use in next-generation electronic devices, particularly as a channel material in field-effect transistors (FETs) and switching devices. Our findings not only enrich the growing library of 2D materials but also pave the way for further research into the device applications of Bi_2C_3 and other members of the M_2C_3 family.

Acknowledgments

This research is funded by Vietnam National Foundation for Science and Technology Development (NAFOSTED) under Grant Number 103.01-2024.14.

References

[1] K. S. Novoselov, A. K. Geim, S. V. Morozov, D. E. Jiang, Y. Zhang, S. V. Dubonos, I. V. Grigorieva, A. A. Firsov, Electric Field Effect in Atomically Thin Carbon Films, Science, Vol. 306, No. 5696, 2004, pp. 666-669, https://doi.org/10.1126/science.1102896.

[2] A. K. Geim, K. S. Novoselov, The Rise of Graphene, Nature Materials, Vol. 6, 2007, pp. 183-191, https://doi.org/10.1038/nmat1849.

[3] Y. Wu, K. A. Jenkins, A. V. Garcia, D. B. Farmer, Y. Zhu, A. A. Bol, C. Dimitrakopoulos, W. Zhu, F. Xia, P. Avouris, State-of-the-Art Graphene High-Frequency Electronics, Nano Letters, Vol. 12, No. 6, 2012, pp. 3062-3067, https://doi.org/10.1021/nl300904k.

[4] F. Bonaccorso, Z. Sun, T. Hasan, A. C. Ferrari, Graphene Photonics and Optoelectronics, Nature Photonics, Vol. 4, 2010, pp. 611-622, https://doi.org/10.1038/nphoton.2010.186.

[5] M. Sun, S. Wang, Y. Liang, C. Wang, Y. Zhang, H. Liu, Y. Zhang, L. Han, Flexible Graphene Field-Effect Transistors and Their Application in Flexible Biomedical Sensing, Nano-Micro Letters, Vol. 17, 2025, pp. 34, https://doi.org/10.1007/s40820-024-01534-x.

[6] S. Manzeli, D. Ovchinnikov, D. Pasquier, O. V. Yazyev, A. Kis, 2D Transition Metal Dichalcogenides, Nature Reviews Materials, Vol. 2, 2017, pp. 1-15, https://doi.org/10.1038/natrevmats.2017.33.

[7] M. Batmunkh, M. B. Erdene, J. G. Shapter, Phosphorene and Phosphorene-Based Materials-Prospects for Future Applications, Advanced Materials, Vol. 28, No. 39, 2016, pp. 8586-8617, https://doi.org/10.1002/adma.201602254.

[8] M. Naguib, M. W. Barsoum, Y. Gogotsi, Ten Years of Progress in the Synthesis and Development of MXenes, Advanced Materials, Vol. 33, No. 39, 2021, pp. 2103393, https://doi.org/10.1002/adma.202103393.

[9] K. F. Mak, C. Lee, J. Hone, J. Shan, T. F. Heinz, Atomically Thin MoS_2: a New Direct-Gap Semiconductor, Physical Review Letters, Vol. 105, 2010, pp. 136805, https://doi.org/10.1103/PhysRevLett.105.136805.

[10] B. Radisavljevic, A. Radenovic, J. Brivio, V. Giacometti, A. Kis, Single-Layer MoS_2 Transistors, Nature Nanotechnology, Vol. 6, 2011, pp. 147-150, https://doi.org/10.1038/nnano.2010.279.

[11] M. Zhang, G. M. Biesold, Z. Lin, A Multifunctional 2D Black Phosphorene-Based Platform for Improved Photovoltaics, Chemical Society Reviews, Vol. 50, No. 23, 2021, pp. 13346-13371, https://doi.org/10.1039/D1CS00847A.

[12] W. Zhang, X. Zhang, L. K. Ono, Y. Qi, H. Oughaddou, Recent Advances in Phosphorene: Structure, Synthesis, and Properties, Small, Vol. 20, No. 4, 2024, pp. 2303115, https://doi.org/10.1002/smll.202303115.
[13] P.-F. Liu, T. Bo, Z. Liu, O. Eriksson, F. Wang, J. Zhao, B.-T. Wang, Hexagonal M_2C_3 (M = As, Sb, and Bi) Monolayers: New Functional Materials with Desirable Band Gaps and Ultrahigh Carrier Mobility, Journal of Materials Chemistry C, Vol. 6, No. 46, 2018, pp. 12689-12697, https://doi.org/10.1039/C8TC04165B.
[14] C. V. Nguyen, P. T. Truong, L. M. Duc, H. V. Phuc, N. V. Hieu, T. P. Linh, N. T. Hiep, C. Q. Nguyen, N. N. Hieu, Interface Engineering and Electric Contact Design of van der Waals Goldene/As_2C_3 Heterostructure for Flexible Electronics, Langmuir, Vol. 41, No. 32, 2025, pp. 21768-21779, https://doi.org/10.1021/acs.langmuir.5c02779.
[15] V. Kumar, D. Azhikodan, D. R. Roy, 2D Sb_2C_3 Monolayer: a Promising Material for the Recyclable Gas Sensor for Environmentally Toxic Nitrogen-Containing Gases (NCGs), Journal of Hazardous Materials, Vol. 405, 2021, pp. 124168, https://doi.org/10.1016/j.jhazmat.2020.124168.
[16] J. Hafner, Ab-Initio Simulations of Materials Using VASP: Density-Functional Theory and Beyond, Journal of Computational Chemistry, Vol. 29, No. 13, 2008, pp. 2044-2078, https://doi.org/10.1002/jcc.21057.
[17] G. Kresse, D. Joubert, From Ultrasoft Pseudopotentials to the Projector Augmented-Wave Method, Physical Review B, Vol. 59, 1999, pp. 1758, https://doi.org/10.1103/PhysRevB.59.1758.
[18] J. P. Perdew, K. Burke, M. Ernzerhof, Perdew, Burke, and Ernzerhof Reply, Physical Review Letters, Vol. 80, 1998, pp. 891-891, http://10.1103/PhysRevLett.80.891.
[19] J. Heyd, G. E. Scuseria, Efficient Hybrid Density Functional Calculations in Solids: Assessment of the Heyd-Scuseria-Ernzerhof Screened Coulomb Hybrid Functional, Journal of Chemical Physics, Vol. 121, No. 3, 2004, pp. 1187-1192, https://doi.org/10.1063/1.1760074.
[20] V. Kumar, K. Rajput, D. R. Roy, Monolayer Bi_2C_3: A Promising Sensor for Environmentally Toxic NCGs with High Sensitivity and Selectivity, Applied Surface Science, Vol. 534, 2020, pp. 147609, https://doi.org/10.1016/j.apsusc.2020.147609.
[21] K. S. Novoselov, A. K. Geim, S. V. Morozov, D. Jiang, M. I. Katsnelson, I. V. Grigorieva, S. V. Dubonos, A. A. Firsov, Two-Dimensional Gas of Massless Dirac Fermions in Graphene, Nature, Vol. 438, 2005, pp. 197-200.
[22] D. C. Wallace, Lattice Dynamics and Elasticity of Stressed Crystals, Reviews of Modern Physics, Vol. 37, 1965, pp. 57, https://doi.org/10.1103/RevModPhys.37.57.
[23] F. Mouhat, F. X. Coudert, Necessary and Sufficient Elastic Stability Conditions in Various Crystal Systems, Physical Review B, Vol. 90, 2014, pp. 224104, https://doi.org/10.1103/PhysRevB.90.224104.
[24] B. Zhang, L. Zhang, N. Yang, X. Zhao, C. Chen, Y. Cheng, I. Rasheed, L. Ma, J. Zhang, 2D Young's Modulus of Black Phosphorene with Different Layers, The Journal of Physical Chemistry C, Vol. 126, No. 2, 2022, pp. 1094-1098, https://doi.org/10.1021/acs.jpcc.1c10187.
[25] C. Lee, X. Wei, J. W. Kysar, J. Hone, Measurement of the Elastic Properties and Intrinsic Strength of Monolayer Graphene, Science, Vol. 321, No. 5887, 2008, pp. 385-388, http://10.1126/science.1157996.
[26] H. Şahin, S. Cahangirov, M. Topsakal, E. Bekaroglu, E. Akturk, R. T. Senger, S. Ciraci, Monolayer Honeycomb Structures of Group-IV Elements and III-V Binary Compounds: First-Principles Calculations, Physical Review B, Vol. 80, 2009, pp. 155453.
[27] F. Tan, J. Li, X. Fang, L. Guan, The Optical Properties of Few-Layer MoS_2 by DFT Calculations, Physica E, Vol. 155, 2024, pp. 115813, https://doi.org/10.1016/j.physe.2023.115813.
[28] A. Maniyar, S. Choudhary, Visible Region Absorption in TMDs/Phosphorene Heterostructures for Use in Solar Energy Conversion Applications, RSC Advances, Vol. 10, No. 53, 2020, pp. 31730-31739, https://doi.org/10.1039/D0RA05810F.
[29] T. Chu, H. Ilatikhameneh, G. Klimeck, R. Rahman, Z. Chen, Electrically Tunable Bandgaps in Bilayer MoS_2, Nano Letters, Vol. 15, No.12, 2015, pp. 8000-8007, https://doi.org/10.1021/acs.nanolett.5b03218.
[30] D. Li, J. R. Xu, K. Ba, N. Xuan, M. Chen, Z. Sun, Y. Z. Zhang, Z. Zhang, Tunable Bandgap in Few-Layer Black Phosphorus by Electrical Field, 2D Materials, Vol. 4, No.3, 2017, pp. 031009, http://10.1088/2053-1583/aa7c98
[31] C. V. Nguyen, P. T. Truong, H. V. Phuc, C. Q. Nguyen, N. T. Hiep, N. N. Hieu, Rationally Designed Versatile Heterostructures Consisted of Two-Dimensional Goldene and MXene Sc_2CF_2, Nano Letters, Vol. 25, No. 26, 2025, pp. 10673-10679, https://doi.org/10.1021/acs.nanolett.5c02560.